

# Robust Conservation Voltage Reduction Evaluation Using Soft Constrained Gradient Analysis

Zixiao Ma<sup>ID</sup>, *Graduate Student Member, IEEE*, Yingmeng Xiang, *Member, IEEE*,  
and Zhaoyu Wang<sup>ID</sup>, *Senior Member, IEEE*

**Abstract**—Evaluation of conservation voltage reduction (CVR) factor is critical to peak load reduction, 556 energy conservation, and many CVR-related power system control/optimization strategies. This paper proposes a novel robust CVR factor evaluation method using soft constrained gradient analysis based on time-varying load modeling and real utility field measurements. Firstly, the time-varying ZIP parameter identification is formulated as an over-determinant problem composed of first-order gradient with respect to each coefficient and soft constraints representing temporal correlation of loads in each time step, in order to improve the robustness and smoothness of CVR factor evaluation. Then, problems in time series are coordinated with a sliding window approach. A necessary condition for selecting the smallest window size is proposed and strictly proved to guarantee the existence and uniqueness of the solution of time-varying load modeling problem. Finally, time-varying CVR factors are accurately and robustly calculated with field measurements and the identified load model. Case studies are performed using sufficient field measurements obtained from two real utilities. Unlike existing methods that require a large number of measurements to obtain precise estimation of CVR factor, the proposed method is sufficiently accurate even when the measurements are limited or of low time resolution. Further, the accuracy and robustness of the proposed approach are validated under different types of uncertainties and compared with other existing data processing and CVR factor evaluation methods.

**Index Terms**—Conservation voltage reduction, time-varying load modeling, robust evaluation, limited measurements.

## NOMENCLATURE

### A. Abbreviations

CVR	Conservation voltage reduction
ANSI	American national standards institute
SVR	Support vector regression
ZIP	Constant impedance, constant current and constant power load
PMU	Phasor measurement unit
WAMS	Wide area management system
SCADA	Supervisory control and data acquisition

Manuscript received 18 June 2021; revised 20 November 2021; accepted 23 January 2022. Date of publication 27 January 2022; date of current version 20 October 2022. This work was supported in part by the U.S. Department of Energy Wind Energy Technologies Office under Grant DE-EE0008956 and in part by the National Science Foundation under Grant ECCS 1929975. Paper no. TPWRS-00971-2021. (Corresponding author: Zhaoyu Wang.)

The authors are with the Department of Electrical and Computer Engineering, Iowa State University, Ames, IA 50011 USA (e-mail: zma@iastate.edu; yingmengxiang@gmail.com; wzy@iastate.edu).

Color versions of one or more figures in this article are available at <https://doi.org/10.1109/TPWRS.2022.3146842>.

Digital Object Identifier 10.1109/TPWRS.2022.3146842

MAD	Median absolute deviation
MSE	Mean squared error
RLS	Recursive least square
RLS-VFF	Recursive least square with variable forgetting factors
MAPE	Mean absolute percentage error
SNR	Signal-to-noise ratio
<i>B. Parameters</i>	
$P_{exp}$	Active power of exponential load model
$k_{exp}$	Exponential load model coefficient
$P_{ZIP}$	Active power of ZIP load model
$P_0$	Nominal active power
$\alpha_P$	Constant impedance coefficient of active power
$\beta_P$	Constant current coefficient of active power
$\gamma_P$	Constant power coefficient of active power
$V$	Voltage magnitude measurement
$V_0$	Nominal voltage
$\mu, \sigma, l$	Median value, standard deviation, and length of the window in Hampel filter
$L$	Total time length of the data set
$n$	Window size
$s$	Number of repetitive data in a window
$\varepsilon_1$	Weight of current initial estimation
$\varepsilon_2$	Weight of historical solution
$\Delta T, T$	Sampling interval and length of data set
$\Delta E$	Saved energy consumption
<i>C. Variables</i>	
$\alpha_{P,t}, \beta_{P,t}, \gamma_{P,t}$	Time-varying coefficients of ZIP model
$P_{ZIP,t}, V_t$	Time-varying active and voltage measurements
$P_t^*$	Active power estimated by load model
$e_t$	Error between power measurement and estimated result
$J$	Accumulative squared error
$V'_t, P'_t$	Rated voltage and power measurements
$A_{\Sigma,t}, A_t, B_{\Sigma,t}$	Matrices of determinant problem
$A_{\varepsilon,t}, B_{\varepsilon,t}$	Matrices of over-determinant problem
$\alpha_{P,t}^o, \beta_{P,t}^o, \gamma_{P,t}^o$	Initial estimation of ZIP coefficients
$CVR_{f,t}^P$	CVR factor for active power at time $t$
$P_{cvroff,t}, P_{cvron,t}$	Active power when CVR is off and on
$V_t, cvroff, V_t, cvron$	Voltage when the CVR is off and on

#### D. Functions

$R(A)$	Range space of $A$
$N(A)$	Kernel of $A$

## I. INTRODUCTION

**A**s a cost-effective way to reduce peak load, save energy and maximize the utilization of power distribution capability, conservation voltage reduction (CVR) is widely studied [1]–[2]. With the integration of distributed renewable energy and electric vehicles in recent years, CVR is becoming increasingly popular in active distribution networks to alleviate the related voltage and energy issues [3]–[4]. According to the American National Standards Institute (ANSI) standard C84.1, the user-end voltage level should be within  $120 \text{ V} \pm 5\%$  [5]. The principle of CVR is to supply the power to the customers at a lower voltage (i.e.,  $114 \text{ V} - 120 \text{ V}$ ) without interrupting the customers. In other countries, there are also similar standards that serve as the lawful foundation of CVR.

The CVR has been implemented by multiple utilities worldwide, such as American Electric Power System, BC Hydro, and Dominion Virginia Power [6]–[7]. From the utilities' point of view, it would be helpful for deciding which feeders are suitable to implement the CVR to achieve best energy saving, if there is an effective method to evaluate the performance of CVR of each feeder. By practical tests conducted by utilities in the past 30 years, they have found that generally  $0.3\% \sim 1\%$  load consumption reduction can be achieved per 1% voltage decrease [7]. This relationship is captured by CVR factor, which is defined as percentile load consumption reduction divided by percentile voltage reduction. Higher CVR factor of a feeder indicates higher energy saving efficiency if CVR is implemented on that feeder. While it brings a lot of benefits to implement the CVR, the detailed CVR factor evaluation should be carefully conducted to aid the operators' decision-making. Actually, multiple challenges are confronting the CVR factor evaluation: 1) the CVR factor depends on a variety of factors, including the power grid configurations, load types, customers' behaviors, local weather, etc., making the CVR factor highly stochastic and time-variant; 2) the integration of distributed generators, microgrids, electric vehicles, and demand response strategies are transforming the distribution systems to be more active, which are complicating the CVR factor evaluation; 3) the CVR factor may be susceptible to or even masked by the natural variation of loads, as well as outliers and noises in the measurement data. Thus, the accurate and robust evaluation of the CVR factor is regarded as a major barrier in implementing CVR [7].

There have been various methods devoted to the CVR factor evaluation, and they can be categorized into five major categories: comparison-based [8], regression-based [9], synthesis-based [10], perturbation-based [11]–[12] and load-modeling-based [13]. 1) The comparison-based method is to apply the CVR to a feeder while applying the normal voltage to a similar feeder at the same time; or it is to apply CVR to a feeder while applying a normal voltage to the same feeder but at another time with similar load conditions. Then, the CVR factor is approximated by the percentage

difference of energy consumptions in the two cases divided by the percentage voltage difference. Although the comparison method is straightforward, it is difficult to find a similar feeder or a similar load condition in practice. 2) The regression method models the load as a linear/nonlinear function with respect to its impact factors, including voltage, season, temperature, etc. This method is comprehensive, but it usually assumes that the coefficients of impact factors do not change over a long time (monthly to yearly), since the measurements with the same sampling rate of all the impact factors are difficult to obtain. 3) In the synthesis-based method, the CVR factor of individual components (e.g., industrial load, commercial load, residential load) are estimated first, then the overall CVR factor is obtained by integrating the CVR factors and the ratios of individual components. It takes effort to analyze the CVR factors of individual components; also, the results obtained in one feeder may not be applicable to another feeder, which hinders the application of the synthesis-based method. 4) The perturbation-based method is recently developed, and it proactively causes a voltage perturbation using an advanced voltage regulation device (e.g., smart inverter or smart transformer) and record the resultant voltage and load variation with an advanced measurement device, such as a phasor measurement unit (PMU), to calculate the CVR factor. While the perturbation-based method has multiple advantages, it requires extra investment to install the smart transformers and PMUs [14], which may prohibit its wide adoption. 5) The load-modeling-based method evaluates the CVR factor by directly analyzing the power-to-voltage sensitivity with well-established load models, such as exponential and ZIP load models. An advantage of this method is that the CVR factor can be analytically calculated, but a sufficient number of measurements are needed for ensuring the accuracy of the load model.

It is worth noting that, the relationship between power and voltage variations in real systems is mainly manifested as load induced voltage change due to line voltage drop and voltage induced load change attributed to CVR effects [11]. The correlation directions of power and voltage in these two scenarios are opposite. In actual systems, the former scenario widely exists, thus leading to inaccurate real-time CVR factor evaluation, if the load composition and parameters are not updated timely. To overcome this problem, CVR factor evaluation based on time-varying ZIP load modeling is motivated, which adjusts the load composition and parameters in real-time.

Recently, the CVR is widely integrated with various power system optimization and control schemes, such as PV generation control [15]–[17], optimal power flow analysis [18], power loss optimization [19], electric vehicle charging scheduling [20], frequency regulation [21], etc. While those researches broaden the application of CVR, they typically assume that the accurate CVR factor is already known for the feeder/substation. This highlights the importance of CVR factor evaluation.

In our previous work, we have proposed multiple CVR factor assessment approaches. In [22], a multi-stage support vector regression (SVR) method is used to estimate the power consumption without voltage reduction during the CVR. Then, the

CVR factor can be calculated with comparison-based method. This method does not assume any CVR model, but the accuracy highly depends on the prediction performance of SVR. In [23], the CVR factor is calculated based on time-varying load modeling, however, the adopted exponential model intrinsically assumes all the load power to be voltage-sensitive. This assumption is relaxed by replacing the exponential model with ZIP model in [24], i.e., the voltage-insensitive components are aggregated into the constant power term. A robust recursive least square method is proposed to identify the coefficients of the ZIP model but with simulated data only. Moreover, due to its dynamical property, the overshoot and settling time after disturbance exist and highly depend on the parameter setup.

To overcome the remaining challenges of the existing CVR factor evaluation methods, this paper proposes a robust time-varying CVR factor evaluation approach for real utility field measurement. Specially, soft constraints of ZIP parameters with temporal correlation among the sliding time windows are integrated into the time-varying parameter identification process. Since in each time window, the optimization problem is solved in a static manner, the overshoot and settling time issues are fully eliminated. To guarantee the existence and uniqueness of the solution of the optimization problem, a necessary condition of the selection of window size is proposed and mathematically proved. Compared with numerical programming approaches, the proposed soft constraints lead to more robust and smoother results. By incorporating the Hampel filter, the robustness against outliers, disturbances and noises in the raw data is significantly improved. From statistical analysis, the proposed is sufficiently accurate, even using measurement with low time-resolution. Comparative studies and statistical analysis are conducted to validate the advantages of this method.

## II. TIME-VARYING LOAD MODELING

### A. Static Load Modeling

Appropriate load modeling is essential to the assessment of CVR factor. Load modeling means the mathematical representation of the load (e.g., active power and reactive power) in a feeder or load bus concerning the relevant factors (e.g., voltage, frequency, temperature, time). Generally, there are three major categories of load models commonly used: static models, dynamic models, and composite models. Static models represent the power of a feeder or bus during a period of time as functions of the magnitudes of static voltages and frequencies, etc., while neglecting the loads' dynamic process. Dynamic models describe the loads' power as dynamic functions with respect to voltages and frequencies, differential equations are usually adopted to describe the power dynamics in response to disturbances. By combining the static models and dynamic models, composite load models can be formulated [25].

Since the main purpose of CVR factor evaluation is to analyze the performance of energy conservation in power grid steady-state operation when the load voltages are deliberately reduced, it is sufficient to adopt a static load model. Examples of the static load models include the exponential model and ZIP model, which are briefly explained as follows.

*1) Exponential Model:* The exponential model describes the relationship between the power and voltage in the following exponential form,

$$\frac{P_{exp}}{P_0} = \left( \frac{V}{V_0} \right)^{k_{exp}} \quad (1)$$

where  $P_{exp}$  is the power measurement and  $k_{exp}$  is the exponential parameter. The exponential load model is often adopted to characterize the mixed loads, and it captures the load restoration feature. As mentioned above, it is important for a load model to capture the load composition to accurately evaluate CVR factor, due to the wide existence of load induced voltage change, in which, the power and voltage have negative correlation. However, exponential load model intrinsically assumes that all the measured power are voltage-correlated. Therefore, an appropriate load model taking load composition into account is imperative [26]–[28].

*2) ZIP Model:* As one of the most commonly used load models, the ZIP model considers three components, i.e., constant impedance ( $Z$ ), constant current ( $I$ ), and constant power ( $P$ ). The active power of the load is expressed as polynomial terms as follows.

$$\frac{P_{ZIP}}{P_0} = \alpha_P \left( \frac{V}{V_0} \right)^2 + \beta_P \frac{V}{V_0} + \gamma_P \quad (2)$$

where  $P_{ZIP}$  is the active power measurement;  $P_0$  is the nominal active power;  $\alpha_P$ ,  $\beta_P$  and  $\gamma_P$  are the active power-related coefficients of the constant impedance, current, and power components, respectively;  $V$  is the voltage magnitude measurement;  $V_0$  is the nominal voltage. It is worth noting that the underlying nominal impedance and nominal current are omitted in (2), since we use the per unit expression. Unlike exponential load model, the voltage-uncorrelated power is reflected in the constant power term in ZIP model.

Other static load models include frequency-dependent model, LOADSYN model developed by Electric Power Research Institute, which are not introduced here due to page limitation.

### B. Time-Varying Load Modeling

Static load models focus on representing the steady-state relationship between load power and voltage/frequency, and it usually assumes the model coefficients to be constants in a relatively long time period. However, this assumption is vulnerable due to customers' power consumption behavior and switching operation of loads. Moreover, load composition is time-variant and the portion of voltage induced load change caused by CVR needs to be determined in real-time for accurate evaluation. As a result, time-varying load models are imperative to depict the time-varying features of loads.

A time-varying ZIP load model for active power is described as follows [23]–[24],

$$\frac{P_{ZIP,t}}{P_0} = \alpha_{P,t} \left( \frac{V_t}{V_0} \right)^2 + \beta_{P,t} \frac{V_t}{V_0} + \gamma_{P,t} \quad (3)$$

where the measurements  $(P_{ZIP,t}, V_t)$  and coefficients  $(\alpha_{P,t}, \beta_{P,t}, \gamma_{P,t})$  are changing with time  $t$ .

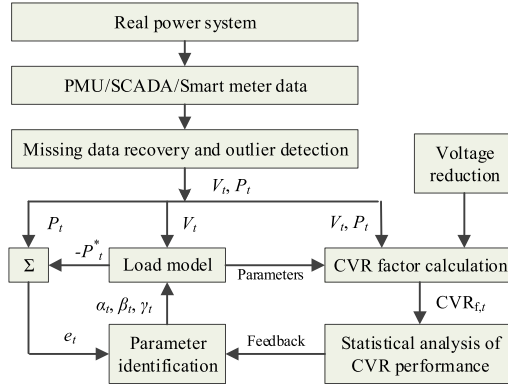


Fig. 1. The overall framework of the proposed CVR evaluation method.

Similarly, a time-varying ZIP load model for reactive power can be derived. They are not explained in detail here since this paper focuses on active power, and the ZIP load model is used as an example of the load models. The proposed method can be conveniently extended to reactive power and other load models.

### III. ROBUST CVR FACTOR EVALUATION

In this section, a robust CVR factor evaluation method is proposed using the time-varying ZIP load modeling and power/voltage field measurement data. A framework of the proposed method is shown in Fig. 1.

In power system long time operation, the measurements, including the active power, reactive power, frequency and voltage, can be continuously obtained by the measurement devices, such as PMUs, smart meters, and/or voltage and current sensors. The measurements for a feeder, for example, can be utilized to model the load characteristics and perform CVR analysis of that feeder. The raw data usually contains some noises or even errors, and part of the data may be missing; thus, appropriate missing data recovery, outlier detection and noise canceling should be implemented. Based on the errors  $e_t$  between the power measurements  $P_t$  and simulated results  $P_t^*$  of the load model, the parameter identification algorithm can update the time-varying coefficients  $(\alpha_{P,t}, \beta_{P,t}, \gamma_{P,t})$  of the load model. When the errors are sufficiently small, the parameters can be finally obtained and sent to the CVR factor calculator. Then, the time-varying CVR factor can be computed with the desired voltage reduction, power and voltage measurements, and identified load model parameters. A statistical analysis is conducted for the calculated CVR factors as feedback to evaluate the accuracy of the methods.

#### A. Raw Data Processing

The power and voltage data needed for CVR factor evaluation can be measured by the PMU devices and transmitted to the control centers via the wide area management system (WAMS) network, or they can be measured by the sensors/meters and transmitted to the control center via the supervisory control and data acquisition (SCADA) network. During both data generation and data transmission processes, errors and noises are inevitable,

which may cause missing and errors in the data received by the control center. Thus, data recovering is needed to recover the missing data if possible; outlier detection should be adopted to replace the outliers with reasonable measurements; filtering should be carried out for the purpose of smoothing the data.

Missing data recovery is an extensively studied topic, and there are a variety of methods available; thus, the missing data recovery is not discussed in detail here. For the outlier detection and data smoothing, the Hampel filter is adopted in this study. It has two parameters to be configured, i.e., the sliding window size and the standard deviation. In the Hampel filter, each data point together with  $l$  points on its both sides in the time series form a data window. The median value  $\mu_i$  of the  $i$ th data window is calculated by

$$\mu_i = \text{median}(x_{i-l}, \dots, x_i, \dots, x_{i+l}) \quad (4)$$

where  $x$  denotes data points. The standard deviation  $\sigma$  is estimated using the median absolute deviation (MAD), i.e.,

$$\sigma_i = 1.4826 \times \text{MAD}_i \quad (5)$$

$$\text{MAD}_i = \text{median}(|x_{i-l} - \mu_i|, \dots, |x_i - \mu_i|, \dots, |x_{i+l} - \mu_i|) \quad (6)$$

Any data point  $x_i$  outside of  $\mu_i \pm 3\sigma_i$  (99.73% confidence level) will be identified as an outlier and replaced with  $\mu_i$ . The window size is selected empirically as 15 in this study for the best performance.

#### B. Problem Formulation of Load Modeling

The CVR factor evaluation is based on the time-varying ZIP model in this paper, and the accuracy of load modeling-based CVR factor assessment approaches highly depends on the performance of parameter identification of the load model. Therefore, to identify the accurate load model parameters, a general optimization problem is formulated to find the optimal coefficients  $\alpha_{P,t}$ ,  $\beta_{P,t}$ , and  $\gamma_{P,t}$  to minimize the accumulative squared error between estimated power and real power using field voltage  $V_t$  and power measurements  $P_t$ .

$$\begin{aligned} & \min_{\alpha_{P,t}, \beta_{P,t}, \gamma_{P,t}} J \\ &= \sum_{t=1}^L \left( \alpha_{P,t} \left( \frac{V_t}{V_0} \right)^2 + \beta_{P,t} \frac{V_t}{V_0} + \gamma_{P,t} - \frac{P_t}{P_0} \right)^2 \end{aligned} \quad (7)$$

$$\text{s.t. } 0 < \alpha_{P,t}, \beta_{P,t}, \gamma_{P,t} < 1 \quad (8)$$

where  $J$  is the accumulative squared error, and  $L$  is the total time length.

#### C. Time-Varying Load Parameter Identification

Since the objective function in (7) is convex, without considering the constraints, the optimum can be calculated by letting the first-order gradient with respect to each of the coefficients

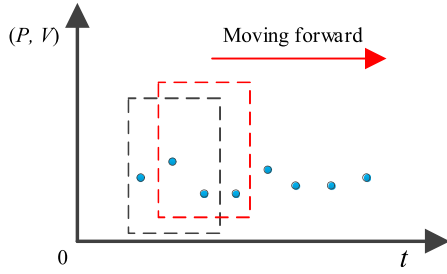


Fig. 2. Schematic of sliding window method.

$\alpha_{P,t}$ ,  $\beta_{P,t}$ ,  $\gamma_{P,t}$  be zero:

$$\frac{\partial J}{\partial \alpha_{P,t}} = \sum_{t=1}^L 2(V_t')^2 (\alpha_{P,t}(V_t')^2 + \beta_{P,t}V_t' + \gamma_{P,t} - P_t') = 0 \quad (9)$$

$$\frac{\partial J}{\partial \beta_{P,t}} = \sum_{t=1}^L 2V_t' (\alpha_{P,t}(V_t')^2 + \beta_{P,t}V_t' + \gamma_{P,t} - P_t') = 0 \quad (10)$$

$$\frac{\partial J}{\partial \gamma_{P,t}} = \sum_{t=1}^L 2(\alpha_{P,t}(V_t')^2 + \beta_{P,t}V_t' + \gamma_{P,t} - P_t') = 0 \quad (11)$$

where we denote  $\frac{V_t}{V_0} = V_t'$  and  $\frac{P_t}{P_0} = P_t'$  for conciseness.

The above problem (9)–(11) is not solvable because it has nine variables but only three equations. A sliding window approach is applied to calculate the time-varying parameters  $\alpha_{P,t}$ ,  $\beta_{P,t}$  and  $\gamma_{P,t}$ , as depicted in Fig. 2. For a set of data in a time window, it is assumed that the time-varying parameters are *constant* in each time window with length  $n$ . Considering discrete-time sampling data, the window moves forward one sampling time's long at a time with overlaps. The calculated parameters within each window are considered as the result of the last sample point of the window, i.e., the parameter identification results start from  $(\alpha_{P,n}, \beta_{P,n}, \gamma_{P,n})$ . Then, denoting  $t' = t - n + 1$ , equations (9)–(11) can be expressed in a matrix form as

$$\begin{bmatrix} \sum_{t=t'}^n V_t'^4 & \sum_{t=t'}^n V_t'^3 & \sum_{t=t'}^n V_t'^2 \\ \sum_{t=t'}^n V_t'^3 & \sum_{t=t'}^n V_t'^2 & \sum_{t=t'}^n V_t' \\ \sum_{t=t'}^n V_t'^2 & \sum_{t=t'}^n V_t' & n \end{bmatrix} \times \begin{bmatrix} \alpha_{P,t'} \\ \beta_{P,t'} \\ \gamma_{P,t'} \end{bmatrix} = \begin{bmatrix} \sum_{t=t'}^n P_t' V_t'^2 \\ \sum_{t=t'}^n P_t' V_t' \\ \sum_{t=t'}^n P_t' \end{bmatrix} \quad (12)$$

where  $t = n, \dots, L$ .

**Theorem 1:** The determinant problem (12) has a unique solution only if  $n - s + 1 \geq 3$ , where  $s \geq 1$  is the number of same-valued/repetitive  $V_t'$  within the window.

**Proof 1:** For conciseness, denote the  $3 \times 3$  matrix on the left-hand-side of (12) as  $A_{\Sigma,t}$ ; denote  $[\alpha_{P,t}, \beta_{P,t}, \gamma_{P,t}]^T$  as  $X_t$ ; denote  $3 \times 1$  vector on the right side of (12) as  $B_{\Sigma,t}$ . We

can have  $A_{\Sigma,t} = \sum_{t=1}^n A_t$  where

$$A_t = \begin{bmatrix} V_t'^4 & V_t'^3 & V_t'^2 \\ V_t'^3 & V_t'^2 & V_t' \\ V_t'^2 & V_t' & 1 \end{bmatrix} \quad (13)$$

Obviously, for each  $t = t', \dots, n$ , the rank of  $A_t$  matrix is 1, denoted as  $\text{rank}(A_t) = 1$ . We know that for  $s$  same-valued  $V_t'$ , it has rank  $(\sum_{t=1}^s A_t) = \text{rank}(sA_t) = \text{rank}(A_t)$ . Since the rank of the sum of  $n$  matrices are less than or equal to the sum of the ranks of each matrix, i.e.,

$$\text{rank}(A_{\Sigma,t}) \leq \sum_{t=1}^n \text{rank}(A_t) = \sum_{t=10}^{n-s+1} \text{rank}(A_t) = n-s+1 \quad (14)$$

Thus, the necessary condition for that  $A_{\Sigma,t}$  has full rank is  $n - s + 1 \geq 3$ . Only under this necessary condition, it is possible to calculate the solution as  $X_t = A_{\Sigma,t}^{-1} B_{\Sigma,t}$ .  $\square$

According to Theorem 1, for each time window with  $n - s + 1 \geq 3$ , i.e., at least three data points with different values, the parameters  $\alpha_{P,t}$ ,  $\beta_{P,t}$  and  $\gamma_{P,t}$  can be calculated by directly solving the determinant problem (12). However, this method has three problems. Firstly, the constraints of parameters  $\alpha_{P,t}$ ,  $\beta_{P,t}$  and  $\gamma_{P,t}$  are not taken into consideration, thus it can overfit the data with abnormal identified parameter values (e.g., the magnitudes of parameters can be hundreds), which leads to meaningless CVR factor evaluation. One popular reason is that the  $n - s + 1$  data points are too similar that leads to singularity. This problem also exists in other unconstrained methods, such as recursive least square (RLS) [23] and robust recursive least square with variable forgetting factors (RLS-VFF) [24]. Secondly, the load variations are mainly driven by human behaviors, environmental weather, and economic activities. All these factors often present temporal correlations. However, the parameter values identified with this method purely depend on the measurements in that window and the temporal correlation with historical data is not considered. Finally, the solution of determinant problem (12) is hypersensitive to the errors and noises in measurement data that are not completely removed by the outlier detection and data smoothing methods, thus leading to weak robustness.

Based on the above reasoning and *Proof 1*, for improving the robustness of time-varying load model parameter identification and capturing the temporal correlation of loads, we propose a method using over-determinant least squares optimization with soft constraints, as shown in (15).

$$\begin{bmatrix} \sum_{t=t'}^n V_t'^4 & \sum_{t=t'}^n V_t'^3 & \sum_{t=t'}^n V_t'^2 \\ \sum_{t=t'}^n V_t'^3 & \sum_{t=t'}^n V_t'^2 & \sum_{t=t'}^n V_t' \\ \sum_{t=t'}^n V_t'^2 & \sum_{t=t'}^n V_t' & n \\ \varepsilon_1 + \varepsilon_2 & 0 & 0 \\ 0 & \varepsilon_1 + \varepsilon_2 & 0 \\ 0 & 0 & \varepsilon_1 + \varepsilon_2 \end{bmatrix} \times \begin{bmatrix} \alpha_{P,t} \\ \beta_{P,t} \\ \gamma_{P,t} \end{bmatrix}$$

$$= \begin{bmatrix} \sum_{t=t'}^n P'_t V_t'^2 \\ \sum_{t=t'}^n P'_t V_t' \\ \sum_{t=t'}^n P'_t \\ \varepsilon_1 \alpha_{P,t}^o + \varepsilon_2 \alpha_{P,t-1} \\ \varepsilon_1 \beta_{P,t}^o + \varepsilon_2 \beta_{P,t-1} \\ \varepsilon_1 \gamma_{P,t}^o + \varepsilon_2 \gamma_{P,t-1} \end{bmatrix} \quad (15)$$

The lower three rows in over-determinant problem (15) softly constrain the values of  $\alpha_{P,t}$ ,  $\beta_{P,t}$  and  $\gamma_{P,t}$  by guiding them towards a near optimal initial estimation that is in the normal range. The initial estimation is a weighted average of two components: solution of current time window  $\alpha_{P,t}^o$ ,  $\beta_{P,t}^o$  and  $\gamma_{P,t}^o$  obtained by solving problem (7)–(8) with interior point method, and the solutions from the last time window,  $\alpha_{P,t-1}$ ,  $\beta_{P,t-1}$  and  $\gamma_{P,t-1}$ . To ensure meaningful CVR factor evaluation,  $\alpha_{P,0}$ ,  $\beta_{P,0}$  and  $\gamma_{P,0}$  must be selected within the normal range [29].  $\varepsilon_1$  and  $\varepsilon_2$  are weighting factors balancing the initial estimation of the current window and the historical solution, respectively. It is worth noting that, the solutions  $\alpha_{P,t}^o$ ,  $\beta_{P,t}^o$  and  $\gamma_{P,t}^o$  are not accurate enough as illustrated in [30], but it can still provide an acceptable initial estimation that serves as soft constraints together with the historical results to guide the time-varying parameter identification.

The over-determinant problem (15) can be solved by the ordinary least squares approach in (16), which gives a unique solution that minimizes the solution errors,

$$X_t = \begin{bmatrix} \alpha_{P,t} \\ \beta_{P,t} \\ \gamma_{P,t} \end{bmatrix} = (A_{\varepsilon,t}^T A_{\varepsilon,t})^{-1} A_{\varepsilon,t}^T B_{\varepsilon,t} \quad (16)$$

where  $A_{\varepsilon,t}$  indicates the  $6 \times 3$  matrix on the left side of (15) and  $B_{\varepsilon,t}$  indicates the  $6 \times 1$  vector on the right side of (15).

**Theorem 2:** The over-determinant problem (15) is guaranteed to have a unique least squares solution as in (16).

**Proof 2:** Since  $A_{\varepsilon,t} X_t$  is an arbitrary vector in the range space of  $A_{\varepsilon,t}$ , i.e.,  $R(A_{\varepsilon,t})$ , the length of the residual vector  $r(X_t) = B_{\varepsilon,t} - A_{\varepsilon,t} X_t$  is the minimal if  $A_{\varepsilon,t} X_t$  is orthogonal to  $R(A_{\varepsilon,t})^\perp$ . Since the orthogonal complement  $R(A_{\varepsilon,t})^\perp = N(A_{\varepsilon,t}^T)$  which is the kernel of  $A_{\varepsilon,t}^T$ ,  $\hat{X}_t$  is a least squares solution if and only if

$$A_{\varepsilon,t}^T r(\hat{X}_t) = 0 \Leftrightarrow A_{\varepsilon,t}^T$$

$$(B_{\varepsilon,t} - A_{\varepsilon,t} \hat{X}_t) = 0 \Leftrightarrow A_{\varepsilon,t}^T A \hat{X}_t = A_{\varepsilon,t}^T B_{\varepsilon,t} \quad (17)$$

It is straightforward to conclude that (17) would have a unique solution if and only if  $A_{\varepsilon,t}^T A_{\varepsilon,t}$  is invertible. Moreover,  $A_{\varepsilon,t}^T A_{\varepsilon,t}$  is invertible if and only if  $A_{\varepsilon,t}$  has full rank.

Importantly, notice that the lower three rows of  $A_{\varepsilon,t}$  are diagonal and full-rank; then,  $A_{\varepsilon,t}$  must have full column rank, which renders (16) and it is guaranteed despite the values of the measurements.  $\square$

Although over-determinant problem (15) is guaranteed to have a unique least squares solution, it is still important to carefully choose the window size  $n$  to ensure the uniqueness of

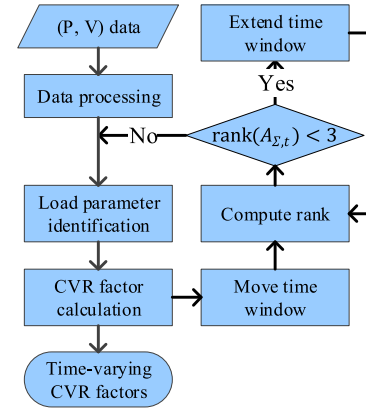


Fig. 3. Flowchart of the proposed CVR factor evaluation method.

$\alpha_{P,t}^o$ ,  $\beta_{P,t}^o$  and  $\gamma_{P,t}^o$ . If  $n$  is too large, it hints that the load model's coefficients should remain unchanged for a long time, which may not be true. If  $n$  is too small (e.g.,  $n = 1$  or 2), the problem (12) does not have a unique solution, as illustrated in *Proof 1*. To balance the strictness of assumption and uniqueness of the solution, the length of the sliding window  $n$  should be selected as small as possible but satisfying  $n - s + 1 \geq 3$ . To ensure the uniqueness of the solution, a variant-window-size method is proposed as follows. To minimize the data requirement, we set  $n = 3$  as a start. Then, the rank of  $A_{\Sigma,t}$  is checked in each sliding window. If  $\text{rank}(A_{\Sigma,t}) < 3$ , extend window size forward to  $n + 1$ , and check the rank again. Repeat this step until  $A_{\Sigma,t}$  has full rank and finally begin the parameter identification. Note that  $A_{\Sigma,t}$  is  $3 \times 3$ , thus the rank checking would not significantly increase computational burden.

#### D. CVR Factor Calculation

The CVR factor is calculated as the percentage of energy reduction over the percentage of voltage reduction. For active power, the CVR factor is obtained as follows,

$$CVR_{f,t}^P = \frac{\Delta P \%}{\Delta V \%} = \frac{P_{cvroff,t} - P_{cvron,t}}{V_{cvroff,t} - V_{cvron,t}} \times \frac{V_{cvroff,t}}{P_{cvroff,t}} \quad (18)$$

$$P_{cvroff,t} = P_0 \left( \alpha_{P,t} \left( \frac{V_{t,cvroff}}{V_0} \right)^2 + \beta_{P,t} \frac{V_{t,cvroff}}{V_0} + \gamma_{P,t} \right) \quad (19)$$

$$P_{cvron,t} = P_0 \left( \alpha_{P,t} \left( \frac{V_{t,cvron}}{V_0} \right)^2 + \beta_{P,t} \frac{V_{t,cvron}}{V_0} + \gamma_{P,t} \right) \quad (20)$$

where  $CVR_{f,t}^P$  is the CVR factor for active power at time  $t$ ;  $P_{cvroff,t}$  and  $P_{cvron,t}$  are the active powers when the CVR is off and on, respectively;  $V_{t,cvroff}$  and  $V_{t,cvron}$  are the voltages when the CVR is off and on, respectively.

Thus, when given a series of power and voltage measurements, the flowchart to calculate the time-varying CVR factors is concluded in Fig. 3.

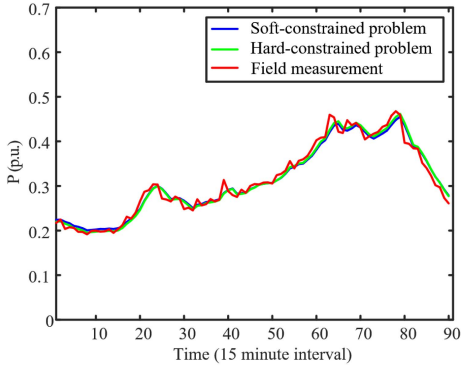


Fig. 4. Comparison of power curves obtained by soft-constrained problem, hard-constrained problem and field measurements.

#### IV. CASE STUDIES

In this section, field measurements from two real utilities on the east coast of the United States are utilized. Multiple case studies are conducted to validate the effectiveness of the proposed soft-constrained gradient analysis based CVR factor evaluation method. The power and voltage measurements for three phases are available, and the three-phase measurements are aggregated for a feeder to calculate its CVR factors.

For a real distribution network with large numbers of feeders, one needs to determine the smallest number of representative feeders before performing CVR factor evaluation on them, in order to reduce computational burden. One cutting-edge method is to use random sampling and clustering methods to find the most representative feeder combination out of the large population of feeders [31]. Note that this paper focuses on improving the accuracy and robustness of CVR factor evaluation method, which is a post-work of the selection of feeders. Therefore, we directly use the feeder data selected by the utilities in the following case studies.

##### A. Comparison Between Determinant Problem and Over-Determinant Problem

To compare the load modeling and CVR factor results between the hard-constrained problem (7)–(8) solved by interior point method and the proposed soft-constrained over-determinant problem (15) solved by the least squares method, the 24-hour data from feeder 1 of substation 1 on September 8 of the year 2012 is selected as an example. The original sampling rate of the field measurement is 4 points per minute. To relax the requirement on the data and to validate that the proposed method is still effective for data with lower sampling rate, the time resolution of the measurements is down-sampled as 15 minutes for this analysis, i.e., one pair of voltage and power data points in the original measurement is selected for every 15 minutes.

As can be seen from Fig. 4, the power curves obtained by the hard-constrained problem and by the soft-constrained problem are both very close to the real field measurements. The mean squared errors are calculated as  $1.64 \times 10^{-4}$  and  $1.50 \times 10^{-4}$ , respectively, which are both sufficiently small.

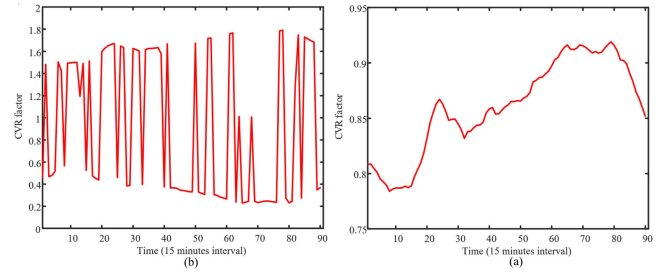


Fig. 5. (a) CVR factor curve of the hard-constrained problem. (b) CVR factor curve of the soft-constrained problem.

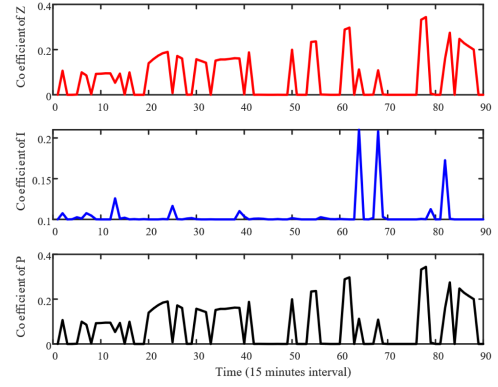


Fig. 6. Curves of the Z, I, P coefficients for the hard-constrained problem.

However, the CVR factors obtained by the hard-constrained problem as shown in Fig. 5(a) are fluctuating violently. They can sharply increase or decrease, or even go out of the appropriate range, which is not reasonable in real practice. On the contrary, the CVR factors obtained by the over-determinant problem, as shown in Fig. 5(b), are varying mildly within the normal range, and there is no sharp increasing or decreasing.

For explaining Fig. 5(a), we check the ZIP coefficients and discover that the sharp fluctuation of the CVR factors of the hard-constrained problem is caused by the sharp fluctuation of identified the ZIP coefficients. As can be observed from Fig. 6, the ZIP coefficients of the hard-constrained problem are fluctuating violently, since they are susceptible to errors and outliers. Different from the hard-constrained problem, the ZIP coefficients solved from soft-constrained over-determinant problem are smoother as shown in Fig. 7. The improvement is attributed to the consideration of temporal correlation modeled by the soft constraints. These comparisons demonstrate the robustness of the proposed soft-constrained over-determinant problem-based approach for CVR factor evaluation.

##### B. Temporal Statistical Analysis

The analysis based on more data is needed to present statistical analysis of the CVR results. Thus, we take more data of the feeder 1 of substation 1 from September 1<sup>st</sup> to November 30<sup>th</sup> in 2012. After discarding the days with measurement errors or meter's shut-down, we screen out 55 days. The ZIP load modeling and the CVR factor calculation are conducted using the data with a time resolution of 15 minutes.

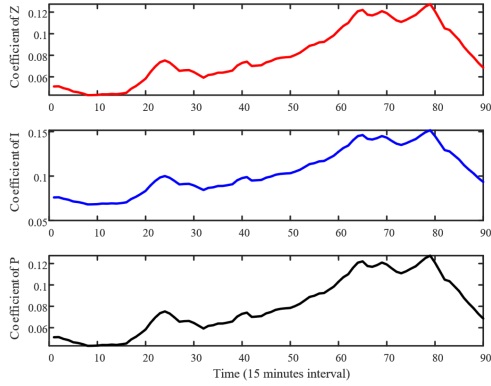


Fig. 7. Curves of the Z, I, and P coefficients for the soft-constrained problem.

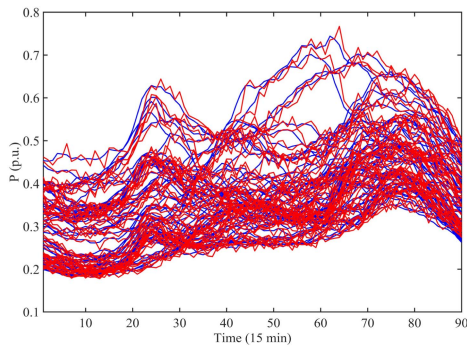


Fig. 8. Identification results using the proposed load modeling approach. The red lines denote the real data and the blue lines denote the estimated power.

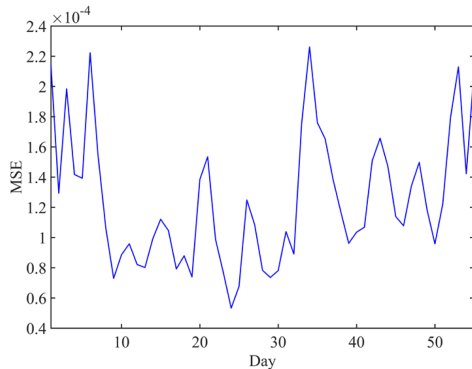


Fig. 9. The mean squared error of the identification result.

The obtained power results of the 55 days are shown in Fig. 8, and each line represents the results for one day. The mean squared error (MSE) of active power of each day is shown in Fig. 9. It can be seen that the errors are small enough.

The CVR factors are then calculated as shown in Fig. 10. It can be seen that the CVR factors vary with time because of the load consumption patterns, and there are no unwanted sharp variations as observed in Fig. 5(a). The CVR factors' statistical analysis is shown in Fig. 11. Empirically, the CVR factors in the temporal statistical analysis should roughly follow a Gaussian distribution [24], and a clear pattern of Gaussian distribution is observed in Fig. 11, which can validate the effectiveness of the proposed CVR estimation approach.

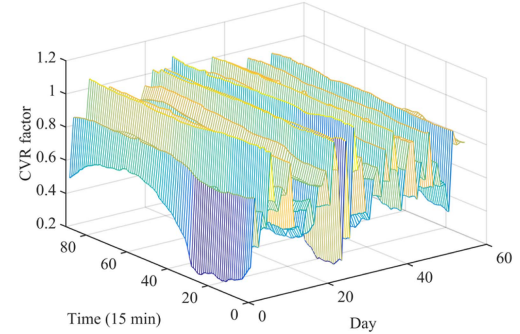


Fig. 10. 3D plot of CVR factor with respect to day and time of substation 1 feeder 1 located on east coast.

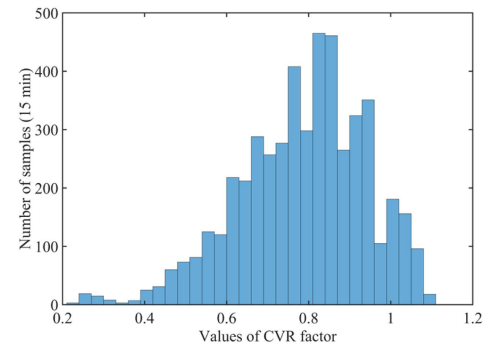


Fig. 11. Histogram of CVR factors of all the data points of substation 1 feeder 1 located on the east coast.

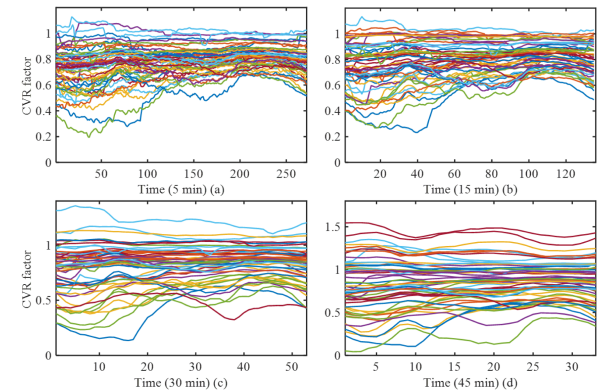


Fig. 12. Comparison of all CVR factor curves of substation 1 feeder 1 for time resolution = 5, 15, 30, and 45 mins.

### C. Influence of Time Resolution on Statistical Analysis

In real practice, the power and measurements may be available with different time resolutions due to various measurement devices and data processing methods adopted. Thus, it is meaningful to check the influence of time resolution of measurement data on the CVR factor calculation.

Simulations are conducted for the measurements with time resolutions of 5, 15, 30, 45 mins, respectively. The calculated CVR curves and histograms are shown in Fig. 12 and Fig. 13, respectively. As can be seen that all the CVR factors fall within the reasonable range, but the standard deviation becomes larger as the time resolution decreases. Because analysis with a low

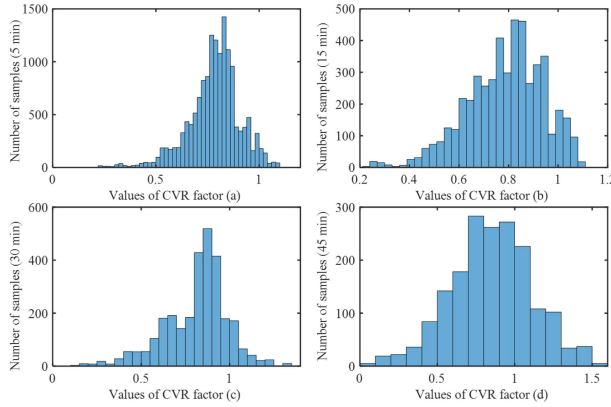


Fig. 13. Comparison of histograms of CVR factors of substation 1 feeder 1 for time resolution = 5, 15, 30, and 45 minutes.

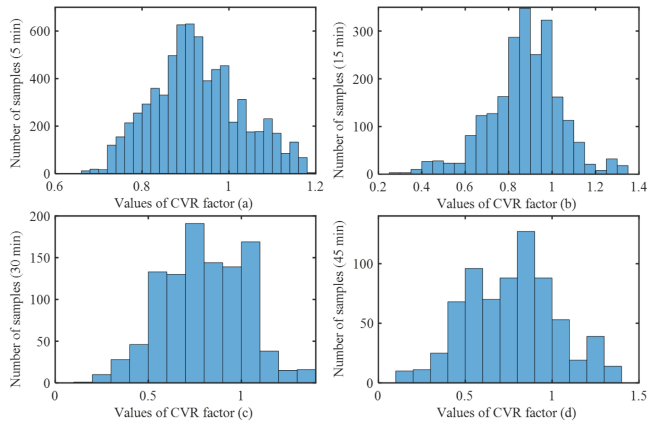


Fig. 14. Comparison of histograms of CVR factors of substation 4 feeder 2 for time resolution = 5, 15, 30, and 45 minutes.

time resolution (e.g., 45 mins) needs the load consumption pattern to keep constant for a long time (e.g., 135 mins if  $n = 3$  data points are used for each CVR factor calculation), which may rarely happen. Thus, it is suggested that CVR factors should be calculated with measurements of a higher time resolution, if possible, as this can lead to more accurate and robust CVR results, especially in the statistical sense.

#### D. Influence of Geographical Location on Statistical Analysis

More CVR factor analyses are carried out in other locations. Take feeder 2 of substation 4 from another utility as an example, 59 days are screened out from August 28<sup>th</sup> to October 25<sup>th</sup>, 2012. The calculated CVR factors are shown in Fig. 14. For different time resolutions, the CVR factor evaluation results still basically follow the Gaussian distributions, which demonstrates that our proposed CVR calculation method is generic and not limited to the data in a particular location.

#### E. Application of CVR Factor to Energy-Saving

As the energy crisis intensifies, the CVR as an effective energy-saving technique becomes more practically valuable. CVR factor evaluation enables operators to predict accurate

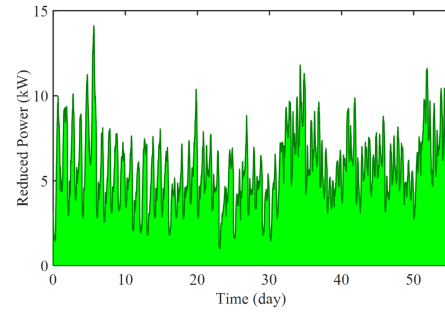


Fig. 15. Reduced power of feeder 1 of substation 1 if CVR is implemented.

energy-saving for a desired voltage reduction, thus helping with decision-making problems, e.g., Volt-VAR optimization [4], [12], [21]. In these problems, the decision variable voltage is computed based on CVR factor, and the accuracy of CVR factor evaluation has great impact on the energy-saving performance. Detailed implementation of the decision-making problems is out of the scope of this paper.

In order to concisely illustrate the practical value of CVR factor evaluation, we test how much energy can be saved for a certain feeder if CVR is implemented on it. To study the effect of CVR in a real power system, we adopt the data set used in Case B which has 55 days of 24-hour continuous field measurement obtained from a real utility. The time resolution of the data is selected as 15 minutes, i.e., CVR factor is evaluated every  $\Delta T = 15$  minutes and held on between each two points. To guarantee voltage safety, the constraint  $V_{cvron,t} \geq 0.95$  is considered when implementing CVR. Then, using the calculated CVR factor, the saved energy consumption  $\Delta E$  can be calculated as

$$\begin{aligned}\Delta E &= \int \Delta P_t dt = \sum_{t=1}^T \Delta P_t \Delta T \\ &= \sum_{t=1}^T CVR_{f,t}^P P_{cvroff,t} \left(1 - \frac{\max\{0.95, V_{cvron,t}\}}{V_{cvroff,t}}\right) \Delta T\end{aligned}$$

where  $T$  denotes the total length of the data set. Fig. 15 shows the time-varying reduced power for 1% voltage reduction. The green area under the reduced power curve denotes the total energy saving on feeder 1 of substation 1 during the 55 days if CVR is implemented, i.e.,  $\Delta E = 7.6$  MWh.

#### F. Robustness Analysis of the Proposed Method

Most types of uncertainties reflected to the  $(P, V)$  data can be classified into outliers, large disturbances and noises. To test the robustness of the proposed method in cases of these uncertainties, three comparison case studies are carried out in this subsection.

*1) Measurement Outliers:* Outliers are usually caused by measurement errors or data loss, and they are replaced by approximated values with Hampel filter in our method. We select the data with outliers of one day at substation 2 feeder 1 to show its influence on the CVR factor. The power curves estimated by ZIP load modeling together with different filters are shown

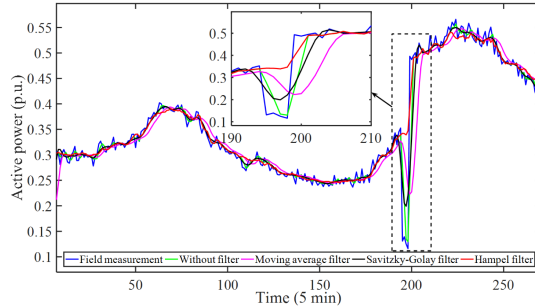


Fig. 16. Comparison of load modeling accuracy with outliers.

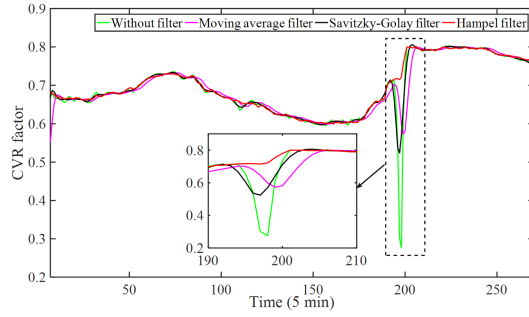


Fig. 17. CVR factors obtained by different filters with outliers.

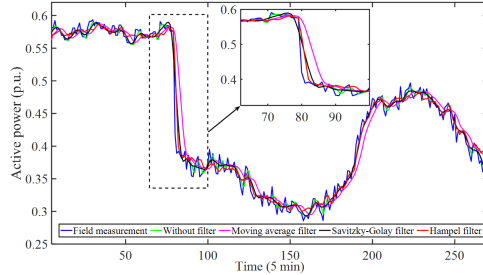


Fig. 18. Comparison of load modeling accuracy with large disturbance.

in Fig. 16, and the corresponding CVR calculation results are shown in Fig. 17. It can be observed that if the Hampel filter is excluded or replaced by moving average filter and Savitzky-Golay filter, the proposed method will indistinctively track the power measurement curve including the outliers; consequently, it will result in outliers of the calculated CVR factors. When the Hampel filter is applied, the robustness of the proposed method against outliers is significantly improved, which validates the necessity of data processing in step 2 of Fig. 3.

2) *Large Disturbance of Load:* Large disturbances are usually caused by load sudden change, switching induced topology change, etc. They should be accurately captured by load modeling but not be removed by robust filters. Similarly, the data with sudden natural load change of one day at substation 2 feeder 1 is selected for robustness analysis. The power curves obtained by ZIP load modeling together with different filters and the related CVR factor calculation results are shown in Figs. 18 and 19, respectively. It shows that the sudden load change will result in a disturbance of the CVR factors, but still in the normal range. After a disturbance, the CVR factor immediately

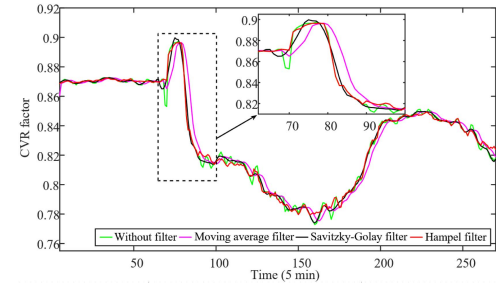


Fig. 19. CVR factors obtained by different filters with large disturbance.

TABLE I  
COMPARISON OF THE THREE ROBUST FILTERS ON DISTURBANCES

Method	Without filter	Moving average	Savitzky-Golay	Hampel
MAPE	0.88%	1.56%	1.00%	0.96%

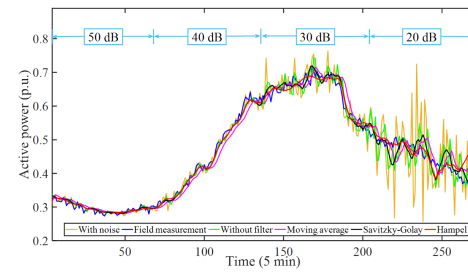


Fig. 20. Comparison of load modeling accuracy with noises.

converges back, which shows the robustness of the proposed algorithm. The accuracy of load modeling is described by mean absolute percentage errors (MAPEs) as shown in Table I. It shows that Hampel filter performs better accuracy than the other two filters especially during the large disturbance, but is slightly less accurate than the result without robust filters. This is because the field measurement contains noises which are filtrated by the Hampel filter, so that the result with Hampel filter is smoother than directly using raw field measurement. The problem of measurement noise is further studied in the next case study.

3) *Noises of Data:* Noises widely exist in field measurements. To study the robustness of the proposed CVR factor evaluation method against noises, white noises with different signal-to-noise ratios (SNRs) are piece-wisely added to a selected field measurement ( $P, V$ ) of substation 2 feeder 1. Note that smaller SNR indicates larger noise magnitude. When  $\text{SNR} \geq 46\text{dB}$ , 99% average percent correct rate is achieved [32]. Therefore, in this case, the tested SNR is selected from 50 dB to 20 dB. Similarly, the performance of Hampel filter is compared with different robust filters. The active power estimated by load modeling with/without different data processing methods are shown in Fig. 20. The corresponding evaluated time-varying CVR factor curves are shown in Fig. 21. The errors between estimated powers and field measurements are quantified as MAPEs in TABLE II. The results show that, the proposed method with Hampel filter is most accurate and has the best robustness against noises in measurements.

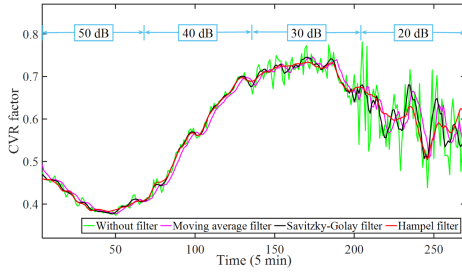


Fig. 21. CVR factors obtained by different filters with noises.

TABLE II  
COMPARISON OF THE THREE ROBUST FILTERS ON NOISES

Method	Without filter	Moving average	Savitzky-Golay	Hampel
MAPE	1.90%	1.86%	1.47%	1.37%

TABLE III  
COMPARISON OF THE THREE LOAD MODELING-BASED CVR FACTOR EVALUATION METHODS

Method	Load model	Robust	Constrained	MAPE
RLS	Exponential	No	No	0.19%
RLS-VFF	ZIP	Yes	No	1.26%
Proposed	ZIP	Yes	Yes	0.36%

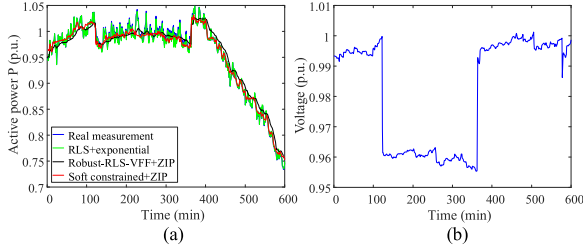


Fig. 22. Comparison of the three load modeling-based CVR factor evaluation methods: (a) Comparison of identification results, (b) Voltage measurement.

### G. Comparison Case Study

The proposed method is compared with two representative load modeling-based time-varying CVR factor evaluation methods: RLS with exponential load model [23] and RLS-VFF with ZIP load model [24]. The three methods are applied to the same field measurement from another utility's substation. To clearly show the difference, we select data with uncertainties on September 24<sup>th</sup>, from 13:00 to 22:59. The sampling rate is 1 data point per minute.

The three methods are compared in Table III. As shown in Fig. 22 and Table III, the load modeling accuracy of the proposed method is a little lower than the conventional RLS method. This is because the field measurement contains noises and the MAPE here is calculated by the error between noisy power measurement and estimated power. The RLS method does not pre-filtrate the noises, thus it undesirably tracks the noisy power and show poorer robustness. The proposed method shows better accuracy than the RLS-VFF method, because the

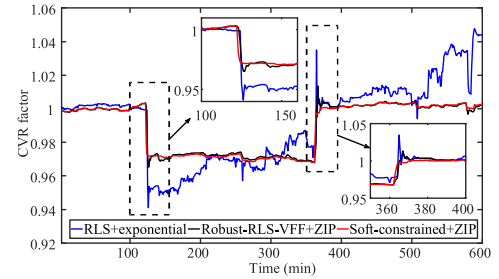


Fig. 23. CVR factors calculated by the three load modeling-based methods.

VFF improves/accelerates the transient performance at some cost of stationary estimation quality [24].

The calculated CVR factors are shown in Fig. 23. The conventional RLS method is not robust enough and it needs longest time to converge when disturbance occurs. Both the proposed soft-constrained method and RLS-VFF method are robust against disturbance, nonetheless, the RLS-VFF method still has some overshooting and requires settling time. Moreover, we can observe that the CVR factor calculated by exponential load model-based method significantly increases after 380 min. This is because the exponential load model intrinsically considers that the power is fully voltage-dependent which leads to over-estimation of CVR factor.

## V. CONCLUSION

A robust time-varying CVR factor evaluation method is proposed in this paper based on the ZIP load model. The first step of the proposed method is processing the raw field measurements to reduce the bad data and noises with a Hampel filter. Then, an over-determinant problem is formulated and solved efficiently to obtain the coefficients of the ZIP load model. A necessary condition for the existence and uniqueness of the solution of the over-determinant problem is proposed and strictly proved. Finally, the CVR factors are calculated based on the ZIP load model, measurements and desired voltage reduction. Based on field measurements from two utilities on the east coast of the USA, case studies are carried out. The studies show that the proposed method is very computationally efficient and easy-to-implement even in cases of low-time-resolution data. An application to energy-saving problem is conducted to show the practical value of CVR factor evaluation. Compared with other existing robust CVR factor evaluation methods, the proposed approach shows the best robustness against uncertainties in the field measurements including large disturbances, outliers and noises.

## REFERENCES

- [1] M. H. K. Tushar and C. Assi, "Volt-VAR control through joint optimization of capacitor bank switching, renewable energy, and home appliances," *IEEE Trans. Smart Grid*, vol. 9, no. 5, pp. 4077–4086, Sep. 2018.
- [2] J. C. Fuller, K. P. Schneider, F. K. Tuffner, and R. Singh, "Evaluation of conservation voltage reduction (CVR) on a national level," U.S. Dept. Energy, Pac. Northwest Nat. Lab., Richland, WA, USA, Rep. PNNL-19596, 2010. [Online]. Available: [http://www.pnl.gov/main/publications/external/technical\\_reports/PNNL-19596.pdf](http://www.pnl.gov/main/publications/external/technical_reports/PNNL-19596.pdf)

- [3] M. T. Rahman, K. N. Hasan, and P. Sokolowski, "Assessment of conservation voltage reduction capabilities using load modelling in renewable-rich power systems," *IEEE Trans. Power Syst.*, vol. 36, no. 4, pp. 3751–3761, Jul. 2021.
- [4] Q. Zhang, K. Dehghanpour, and Z. Wang, "Distributed CVR in unbalanced distribution systems with PV penetration," *IEEE Trans. Smart Grid*, vol. 10, no. 5, pp. 5308–5319, Sep. 2019.
- [5] *ANSI Standard C84.1-1995 Electric Power Systems and Equipment Voltage Ratings (60 Hz)*, ANSI, Arlington, Virginia, USA, National Electrical Manufacturers Association, 1995.
- [6] T. A. Short and R. W. Mee, "Voltage reduction field trials on distribution circuits," in *Proc. IEEE PES Transmiss. Distrib. Conf. Expo.*, 2012, pp. 1–6.
- [7] Z. Wang and J. Wang, "Review on implementation and assessment of conservation voltage reduction," *IEEE Trans. Power Syst.*, vol. 29, no. 3, pp. 1306–1315, May 2014.
- [8] T. J. Krupa and H. Asgeirsson, "The effects of reduced voltage on distribution circuit loads," *IEEE Trans. Power Syst.*, vol. 2, no. 4, pp. 1013–1018, Nov. 1987.
- [9] T. L. Wilson, "Measurement and verification of distribution voltage optimization results," in *Proc. IEEE Power Energy Soc. Gen. Meeting*, 2010, pp. 1–9.
- [10] J. De Steese, S. Merrick, and B. Kennedy, "Estimating methodology for a large regional application of conservation voltage reduction," *IEEE Trans. Power Syst.*, vol. 5, no. 3, pp. 862–870, Aug. 1990.
- [11] J. Xu *et al.*, "Online assessment of conservation voltage reduction effects with micro-perturbation," *IEEE Trans. Smart Grid*, vol. 12, no. 3, pp. 2224–2238, May 2021.
- [12] G. De Carne, S. Bruno, M. Liserre, and M. La Scala, "Distributed online load sensitivity identification by smart transformer and industrial metering," *IEEE Trans. Ind. Appl.*, vol. 55, no. 6, pp. 7328–7337, Dec. 2019.
- [13] M. S. Hossan and B. Chowdhury, "Comparison of time-varying load models for estimating CVR factor and VSF using dual-stage adaptive filter," *IEEE Trans. Power Del.*, vol. 34, no. 3, pp. 1001–1010, Jun. 2019.
- [14] R. R. Jha, A. Dubey, C. Liu, and K. P. Schneider, "Bi-Level Volt-VAR optimization to coordinate smart inverters with voltage control devices," *IEEE Trans. Power Syst.*, vol. 34, no. 3, pp. 1801–1813, May 2019.
- [15] F. Ding and M. Baggu, "Coordinated use of smart inverters with legacy voltage regulating devices in distribution systems with high distributed PV penetration - Increase CVR energy savings," *IEEE Trans. Smart Grid*, early access, Jul. 18, 2018, doi: [10.1109/TSG.2018.2857410](https://doi.org/10.1109/TSG.2018.2857410).
- [16] S. Singh, S. Veda, S. P. Singh, R. Jain, and M. M. Baggu, "Event-driven predictive approach for real-time Volt/VAR control with CVR in solar PV rich active distribution network," *IEEE Trans. Power Syst.*, vol. 36, no. 5, pp. 3849–3864, Sep. 2021.
- [17] R. Cheng, Z. Wang, Y. Guo, and F. Bu, "Analyzing photovoltaic's impact on conservation voltage reduction in distribution networks," in *Proc. North Amer. Power Symp.*, 2021, pp. 1–6.
- [18] L. Gutierrez-Lagos and L. F. Ochoa, "OPF-based CVR operation in PV-rich MV-LV distribution networks," *IEEE Trans. Power Syst.*, vol. 34, no. 4, pp. 2778–2789, Jul. 2019.
- [19] H. Gharaviahangar, L. F. Ochoa, X. Liu, G. Paterson, B. Ingham, and S. Mcloone, "CVR and loss optimization through active voltage management: A trade-off analysis," *IEEE Trans. Power Del.*, vol. 36, no. 6, pp. 3466–3476, Dec. 2021.
- [20] S. Singh, V. B. Pamshetti, and S. P. Singh, "Time horizon-based model predictive Volt/VAR optimization for smart grid enabled CVR in the presence of electric vehicle charging loads," *IEEE Trans. Ind. Appl.*, vol. 55, no. 6, pp. 5502–5513, Dec. 2019.
- [21] Q. Zhang, Y. Guo, Z. Wang, and F. Bu, "Distributed optimal conservation voltage reduction in integrated primary-secondary distribution systems," *IEEE Trans. Smart Grid*, vol. 12, no. 5, pp. 3889–3900, Sep. 2021.
- [22] Z. Wang, M. Begovic, and J. Wang, "Analysis of conservation voltage reduction effects based on multistage SVR and stochastic process," *IEEE Trans. Smart Grid*, vol. 5, no. 1, pp. 431–439, Jan. 2014.
- [23] Z. Wang and J. Wang, "Time-varying stochastic assessment of conservation voltage reduction based on load modeling," *IEEE Trans. Power Syst.*, vol. 29, no. 5, pp. 2321–2328, Sep. 2014.
- [24] J. Zhao, Z. Wang, and J. Wang, "Robust time-varying load modeling for conservation voltage reduction assessment," *IEEE Trans. Smart Grid*, vol. 9, no. 4, pp. 3304–3312, Jul. 2018.
- [25] Z. Ma, B. Cui, Z. Wang, and D. Zhao, "Parameter reduction of composite load model using active subspace method," *IEEE Trans. Power Syst.*, vol. 36, no. 6, pp. 5441–5452, Nov. 2021.
- [26] S. Liao *et al.*, "Load-damping characteristic control method in an isolated power system with industrial voltage-sensitive load," *IEEE Trans. Power Syst.*, vol. 31, no. 2, pp. 1118–1128, Mar. 2016.
- [27] J. Xu *et al.*, "Load shedding and restoration for intentional island with renewable distributed generation," *J. Mod. Power Syst. Clean Energy*, vol. 9, no. 3, pp. 612–624, May 2021.
- [28] M. Diaz-Aguiló *et al.*, "Field-validated load model for the analysis of CVR in distribution secondary networks: Energy conservation," *IEEE Trans. Power Del.*, vol. 28, no. 4, pp. 2428–2436, Oct. 2013.
- [29] P. K. Sen and K. H. Lee, "Conservation voltage reduction technique: An application guideline for smarter grid," *IEEE Trans. Ind. Appl.*, vol. 52, no. 3, pp. 2122–2128, May 2016.
- [30] S. M. H. Rizvi, K. S. Sajan, and A. Srivastava, "Synchrophasor based ZIP parameters tracking using ML with adaptive window and data anomalies," *IEEE Trans. Power Syst.*, vol. 37, no. 1, pp. 3–13, Jan. 2022.
- [31] M. S. Hossan *et al.*, "Deployment of conservation voltage reduction in sample feeders: A systemwide energy-savings analysis," *IEEE Ind. Appl. Mag.*, vol. 27, no. 2, pp. 36–46, Mar./Apr. 2021.
- [32] B. P. Ross, T. J. Carbino, and S. J. Stone, "Physical-layer discrimination of power line communications," in *Proc. Int. Conf. Comput., Netw. Commun.*, 2017, pp. 341–345.



**Zixiao Ma** (Graduate Student Member, IEEE) received the B.S. degree in automation and the M.S. degree in control theory and control engineering from Northeastern University, Boston, MA, USA, in 2014 and 2017, respectively. He is currently working toward the Ph.D. degree with the Department of Electrical and Computer Engineering, Iowa State University, Ames, IA, USA. His research interests include power system load modeling, microgrids, nonlinear control, and model reduction.



**Yingmeng Xiang** (Member, IEEE) received the B.S. degree from Chongqing University, Chongqing, China, in 2010, the M.S. degree from the Huazhong University of Science and Technology, Wuhan, China, in 2013, and the Ph.D. degree from the University of Wisconsin-Milwaukee, Milwaukee, WI, USA, in 2017. He is currently a Postdoctoral Research Associate with Iowa State University, Ames, IA, USA. His research interests include power distribution optimization, IoT for power systems, smart grid reliability, and cyber-physical system resiliency. He is the Editor for the IEEE TRANSACTIONS ON SMART GRID.



**Zhaoyu Wang** (Senior Member, IEEE) received the B.S. and M.S. degrees in electrical engineering from Shanghai Jiao Tong University, Shanghai, China, and the M.S. and Ph.D. degrees in electrical and computer engineering from the Georgia Institute of Technology, Atlanta, GA, USA. He is currently the Northrop Grumman Endowed Associate Professor with Iowa State University, Ames, IA, USA. His research interests include optimization and data analytics in power distribution systems and microgrids. He was the recipient of the National Science Foundation CAREER Award, Society-Level Outstanding Young Engineer Award from IEEE Power and Energy Society (PES), Northrop Grumman Endowment, College of Engineering's Early Achievement in Research Award, and Harpole-Pentair Young Faculty Award Endowment. He is the Principal Investigator for a multitude of projects funded by the National Science Foundation, Department of Energy, National Laboratories, PSERC, and Iowa Economic Development Authority. He is the Chair of IEEE PES PSOPE Award Subcommittee, the Co-Vice Chair of PES Distribution System Operation and Planning Subcommittee, and the Vice Chair of PES Task Force on Advances in Natural Disaster Mitigation Methods. He is an Associate Editor for the IEEE TRANSACTIONS ON POWER SYSTEMS, IEEE TRANSACTIONS ON SMART GRID, IEEE OPEN ACCESS JOURNAL OF POWER AND ENERGY, IEEE POWER ENGINEERING LETTERS, and IET Smart Grid.